Atmospheric Environment 212 (2019) 250–261

Contents lists available at ScienceDirect

Atmospheric Environment

journal homepage: www.elsevier.com/locate/atmosenv

Source apportionment of carbonaceous aerosols in the vicinity of a Mediterranean industrial harbor: A coupled approach based on radiocarbon and molecular tracers

Lise Bonvalot[a,*], Thibaut Tuna[a], Yoann Fagault[a], Alexandre Sylvestre[b,c], BouAlem Mesbah[d], Henri Wortham[b], Jean-Luc Jaffrezo[e], Nicolas Marchand[b], Edouard Bard[a,**]

[a] CEREGE, Aix-Marseille University, CNRS, IRD, INRA, Collège de France, Technopôle de l'arbois, BP 80, 13545, Aix-en-Provence, France
[b] Aix Marseille Univ, CNRS, LCE, Marseille, France
[c] Institut Ecocitoyen pour La Connaissance des Pollutions, 13270, Fos-sur-Mer, France
[d] AtmoSud, Air Quality Observatory in Provence Alpes Côte D'Azur, Marseille, France
[e] Univ. Grenoble Alpes, CNRS, IRD, IGE (UMR 5001), F-38000, Grenoble, France

ARTICLE INFO

Keywords:
$PM_{2.5}$
Radiocarbon
Levoglucosan
Carbonaceous particles
Mediterranean basin

ABSTRACT

Located in the Mediterranean Basin and close to Marseille (France), Fos-sur-Mer is situated in the vicinity of industrial harbor and agricultural lands. Its location makes it prone to mixed pollution contributions, combining the influence of residential, industrial, agricultural, maritime road and traffic sources. For this study, the origins of carbonaceous particles sampled over several months are investigated by a coupled approach based on analyses of radiocarbon (^{14}C), elemental to total carbon ratio (EC/TC) and various molecular tracers (levoglucosan, methoxyphenols, malic and glyceric acids), giving information about their background origins. Accelerator mass spectrometry with a gas ion source give the opportunity to quantify the fossil and non-fossil fractions for each individual sample, avoiding to pool them. Analyzing ^{14}C in micro-samples (down to a few μg of carbon) complements the approach based on chemical tracers, which are useful to identify sources, but insufficient to quantify accurately the modern and fossil carbon fractions.

The measurements in about 30 samples collected during summer and fall/winter 2013, allow the detection of a strong seasonality of the pollution: the fall/winter $PM_{2.5}$ fraction concentration equals to three times the summer concentration and we observe a significant fluctuation of the relative contributions of fossil and non-fossil fractions (f_{NF} is ≈ 0.83 for fall/winter samples and ≈0.59 for summer samples).

Significant correlations between ^{14}C, levoglucosan and different methoxyphenols, allow the identification and quantification of a major influence of biomass burning emissions during fall and winter. Biomass burning organic carbon (OC_{BB}) and elemental carbon (EC_{BB}) contribute to 45% and 8% of the TC, respectively, whereas their total contribution is only 3% in summer samples.

Biogenic emissions from the vegetation are the main sources of carbon during summer (≈57%). Significant correlations between summer OC_{bio} and malic acid and DL glyceric acid suggest a secondary origin for this fraction.

The total fossil carbon concentration (EC_F and OC_F) from vehicular, shipping and industrial sources is constant throughout the year, which is compatible with intense road and maritime traffics and industrial activity during both seasons.

Overall, our study based on ^{14}C and molecular tracers illustrates the power of a coupled approach in order to both identify and quantify biomass burning, biogenic, traffic and industrial sources of carbonaceous aerosols, forming a complex mix of background PM origins in a typical industrious harbor of the Mediterranean region.

* Corresponding author.
** Corresponding author.
E-mail addresses: bonvalot@cerege.fr (L. Bonvalot), bard@cerege.fr (E. Bard).

https://doi.org/10.1016/j.atmosenv.2019.04.008
Received 2 August 2018; Received in revised form 25 March 2019; Accepted 2 April 2019
Available online 06 April 2019

1. Introduction

Atmospheric Particulate Matter (PM) is a challenging environmental issue as it is known to affect the climate on regional and global scales, by reflecting, scattering and absorbing sunlight and by modifying cloud properties (Chung and Seinfeld, 2002; Penner et al., 1998; Ramanathan et al., 2001b, 2001a). Particles also have a direct and harmful effect on human health, causing respiratory and cardiopulmonary diseases (Lelieveld et al., 2019, 2015; Pope and Dockery, 2006), which can lead to an increased mortality. PM can be directly emitted (primary particles) by natural sources (marine, soil dust, or biogenic emissions) or anthropogenic sources (heating, traffic, industry). PM can also be formed from the condensation of oxidized semi volatile species or by heterogeneous liquid phase reaction in the atmosphere (secondary particles). Secondary particles can also originates from the creation of new particles by nucleation process; the quick formation of SOA (Secondary Organic Aerosol) by this process can explain the concentrations obtained in remoted location (Jimenez et al., 2009). The atmospheric aerosols undergo several physical and chemical transformations (aerosol aging) which change the structure and chemical composition of particles. Given that carbonaceous materials have been demonstrated to represent an important proportion of PM in almost all cases (Fuzzi et al., 2015; Pöschl, 2005; Putaud et al., 2010, 2004), determining and apportioning sources of that fraction is an essential step to improve air quality. Of particular difficulty is the accurate quantification of the fossil and non-fossil carbon fractions from small-size PM samples typically recovered in aerosol filters.

In the last years, the OA (Organic Aerosol) sources in the Mediterranean Basin have been increasingly investigated (Arndt et al., 2017; Bozzetti et al., 2017; El Haddad et al., 2013, 2011; 2009; Michoud et al., 2017; Minguillón et al., 2016; Salameh et al., 2015), with the identification of contributions from fossil fuel combustion, from biomass burning (for the cold season) and from shipping. The South of France is a region subjected to abrupt and intense wind episodes (e.g. mistral wind), which can influence the total concentration and the mixing of PM. In the Marseille area, one of the largest harbors along the coasts of the Mediterranean Sea, several studies have also shown the strong influence on aerosols of the photo-oxidation in summer, and of the biomass burning emissions in winter (Bozzetti et al., 2017; Salameh et al., 2015).

The Fos-sur-Mer area is densely populated and is also one of the most industrialized in France. The proximity with the Fos-Berre Industrial Port Zone, (Zone Industrialo-Portuaire: ZIP) leads to complex influences on the atmospheric pollution felt in and around the city of Fos-sur-Mer. In 2008, a study of health risks conducted on the ZIP assessed that about 9000 tons per year of $PM_{2.5}$ originate from industrial emissions, while maritime and road traffic contribute to about 230 and 15 tons per year, respectively (Goix et al., 2017). The regional air quality control association (AtmoSud) recorded that the PM_{10} air quality goal limit (30 $\mu g\,m^{-3}$ annual average) was exceeded for the years 2010 and 2011, illustrating the importance of background PM pollution (Dron et al., 2017).

To determine and quantify the influence of the ZIP from that of others PM sources (from domestic and natural emissions), and to be able to detect sharp and singular pollution events, it is necessary to achieve a good knowledge of the atmospheric PM background. It can be obtained with the chemical analysis of a large data set, covering both winter and summer seasons, and including specific chemical tracers of the several potential sources. The use of chemical tracers (e.g. levoglucosan) allows identifying sources and estimating their relative contributions, but it relies on assumptions about tracer/OA ratios. The analysis of radiocarbon (^{14}C, radioactive carbon isotope) in the carbonaceous fractions of aerosols is a complementary tool, which is the best technique to separate and quantify fossil fuel combustion products from other non-fossil carbon sources, such as biomass burning and biogenic emissions (Currie, 2000; Heal et al., 2011; Szidat et al., 2009, 2006; Bonvalot et al., 2016).

Radiocarbon is continuously and naturally produced in the upper atmosphere by the interaction between secondary neutrons from cosmic rays and nitrogen nuclei from the air. The produced ^{14}C is then oxidized into $^{14}CO_2$ and mixed in the atmosphere. CO_2 (and therefore $^{14}CO_2$) is partly taken up by vegetation during photosynthesis. Living organisms such as plants exhibit $^{14}C/^{12}C$ ratios similar to those of the atmospheric pool (in the order of 10^{-12}). Consequently, biogenic emissions present the same $^{14}C/^{12}C$ ratio as the atmosphere. Emissions from biomass burning present isotopic ratios close to, but slightly higher than the former, due to the increase of atmospheric radiocarbon concentration during the 1950s and 1960s resulting from thermonuclear bomb tests in the atmosphere (Levin et al., 2010, 2013; Hua et al., 2013). As radiocarbon decays with a half-life of 5730 years, fossil fuels made of geological organic matter are totally depleted in ^{14}C. It is thus possible to determine the non-fossil fraction (f_{NF}) and the fossil fraction (f_F) by measuring the radiocarbon in the whole carbonaceous fraction of atmospheric aerosols.

In a series of PM samples from Fos-sur-Mer, we have measured ^{14}C, organic carbon and elemental carbon (OC-EC), and chemical proxies of biomass burning and biogenic emission proxies (levoglucosan, methoxyphenols, malic and glyceric acids). This allows us to determine the origins of the background carbonaceous particles of this industrial area. This better knowledge of chronical pollution sources in Fos-sur-Mer is invaluable in order to be able to detect future punctual pollution events in this region.

2. Methods

2.1. Particulate matter sampling

2.1.1. Location of sampling and aims of the study

Located in the south of France, about 40 km NW from Marseille, in a widely populated area (about 402 000 inhabitants, *i.e.* 311 inhabitants per km^2 (Sylvestre et al., 2017), the city of Fos-sur-Mer is close to the Fos-Berre ZIP.

Sampling was performed in a Fos-sur-Mer residential zone called “les Carabins”, see Fig. 1, (43.45°N, 4.93°E), located close to the ZIP. This sampling site is representative of the urban background air pollution and thus of the inhabitants’ exposure. It is also surrounded by agricultural lands and a French Air Force base, to the east by the “Étang de Berre”, (with a residential area and petrochemical activities), to the south by the Mediterranean Sea, (with a strong maritime traffic, but also some residential areas and petrochemical activities) and to the southwest/south by the ZIP center with its many industrial sources, petrochemical activities, steel industry and maritime traffic.

The field campaign was conducted from May 2012 to August 2013. $PM_{2.5}$ samples were collected daily (24 h per day, starting at 0 h UTC) for the whole period. Briefly, aerosols were collected on 150 mm diameter quartz fiber filters (Pall Corporation Pallflex) with a high-volume sampler (DA80 Digitel, flowrate = 30 $m^3\,h^{-1}$). Quartz filter were baked for 5 h at 500 °C beforehand. However, high volume sampling induces well-characterized collection artifacts such as adsorption but also volatisation and chemical transformation onto the filter during sampling (Goriaux et al., 2006; Mader and Pankow, 2000; Sihabut et al., 2005). Even if high volume samplers limit the organic gaseous compounds adsorption onto the filter, compared to low volume sampler (Kim et al., 2016; Viana et al., 2006), those artifacts can modify the concentrations of some organic compounds. However, high volume samplers are widely used because of their reliability. Artifacts are highly dependent on sampling conditions, such as temperature, air masses ages, sampling time, and corrections are thus difficult to determine and apply.

Further details are presented elsewhere (Sylvestre et al., 2017). The present work is focused on the analysis of carbonaceous particles from a subset of 30 $PM_{2.5}$ samples (from 49 $PM_{2.5}$ samples initially), selected in function of preliminary apportionment results (Sylvestre, 2017);

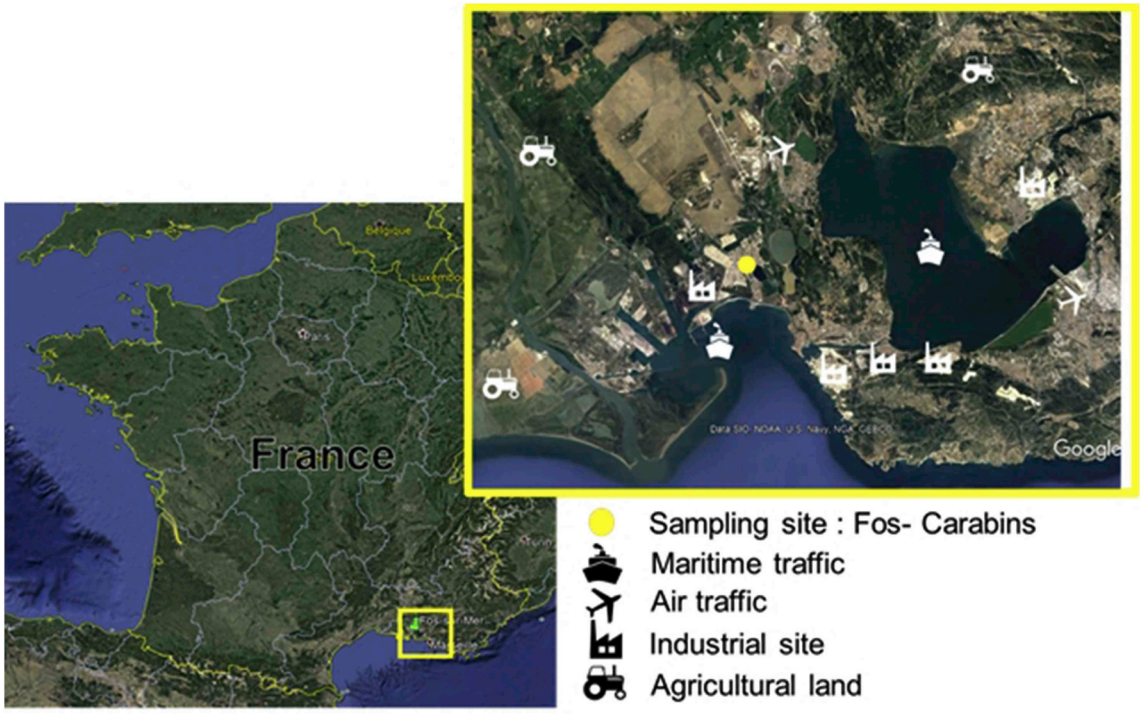

Fig. 1. Location of the sampling site (yellow point) in a residential zone "les Carabins" in Fos-sur-Mer. (For interpretation of the references to color in this figure legend, the reader is referred to the Web version of this article.)

radiocarbon measurements were focused on samples which needed more constrains, to ensure a better PM source attribution with the ME-2 model. More specifically, of the 30 samples, 1 was sampled during the spring of 2012, 20 were sampled during the cold season (fall/winter) of 2012–2013, and the remaining 9 were collected during summer 2013. Even if it is limited due to the cost and difficulty of the gas-source AMS ^{14}C analyses (all being duplicated), this repartition provides a way to estimate the seasonal variation between the warm (spring-summer) and cold season (fall/winter).

2.2. Measurements and analyses

2.2.1. Organic markers

For this study, we used analyses of levoglucosan, methoxyphenols (vanillin, acetovanillone and vanillic acid) malic and glyceric acids are considered.

Levoglucosan is formed during the pyrolysis of cellulose (Simoneit et al., 1999) at temperatures higher than 300 °C (Caseiro et al., 2009). For this reason, levoglucosan is widely used as a biomass burning tracer in source apportionment studies (Dusek et al., 2017; Jordan et al., 2006; Martinsson et al., 2017; Schauer et al., 2001; Waked et al., 2014; Zhang et al., 2008). It is noteworthy that several studies have shown that levoglucosan may not be stable in the troposphere (Hennigan et al., 2010), leading to reduced life time (1–5 days) in the atmosphere, depending on the season and atmospheric conditions. However, the degradation rate of levoglucosan in ambient atmospheric aerosols is yet to be determined precisely (Bertrand et al., 2018b; Yttri et al., 2015).

Methoxyphenols, such as vanillin, acetovanillone and vanillic acid, are emitted by thermal decomposition of lignin and can also be used as BB tracers (Bertrand et al., 2018a; Nolte et al., 2001). Bertrand et al. (2018a,b) classified these methoxyphenols as non-conventional primary compounds because they are emitted both as primary compounds and as secondary compounds during aerosol aging.

Malic and glyceric acids can be used as biogenic SOA markers. Malic acid has been proposed as a late-stage product in the photooxydation process of fatty acids synthesized by plants (Hsieh et al., 2007). It can also originate from the oxidation of n-alkanes emitted by the vegetation (Claeys et al., 2004; Kawamura et al., 1996; Kawamura and Bikkina, 2016). It has been shown that DL-glyceric acid can be produced by the oxidation of diene compounds synthesized by the vegetation (Angove et al., 2006).

These polar organic marker measurements were carried out by gas chromatography (GC) coupled with mass spectrometry (MS). Analytical methods and performances are described elsewhere (El Haddad et al., 2011, 2013; Salameh et al., 2015; Sylvestre et al., 2017; Betrand et al., 2108a, b). Briefly, prior to sample extraction, 300 µL of a solution containing the internal standards (D50-Tetracosane ($C_{24}D_{50}$) and D6-Cholesterol ($C_{24}H_{40}D_{60}$)) were spiked onto the filters. Samples were then extracted using an Accelerated Solvent Extractor (ASE Dionex 300) with a mixture of acetone/dichloromethane (1/1 v/v) at 100 bar and 100 °C during 10 min. Sample extracts were then concentrated using a Turbo Vap II under N_2 in a water-bath regulated at 40 °C. After concentration the final volume of the extracts was 500 µL. A 50 µL fraction of the extracts was derivatized at 70 °C during 90 min by adding 100 µL of N,O-bis(triméthylsilyl)trifluoroacétamide (BSTFA) containing 1% of Trimethychlorosilane, in order to analyze those polar compounds Derivatized extracts were then analyzed using a Thermo Trace Ultra GC coupled with a Polaris Q – ion trap.

2.2.2. OC-EC

OC (Organic Carbon) and EC (Elemental Carbon) were quantified by thermo-optical analysis. A Sunset instrument (Birch and Cary, 1996) running with the EUSAAR_2 method with optical correction of charring performed by transmittance (TOT) (Cavalli et al., 2010) was used to analyze 1.5 cm^2 punches of the sampled filters. Total carbon (TC) is the sum of OC and EC. Those values were also used to determine the EC/TC ratio for each sample. The EC fraction is composed of primary particles only and originates from the combustion process, whereas the OC fraction is more complex and is composed of primary and secondary particles (Gelencsér, 2004; Pöschl, 2005).

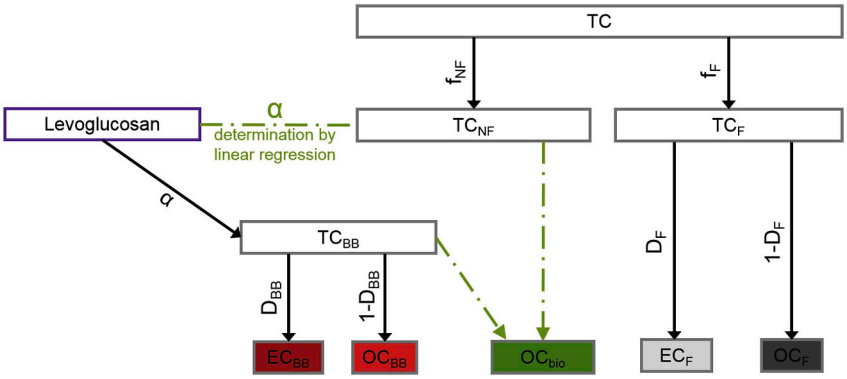

Fig. 2. Representation of the different fractions composing carbonaceous aerosols. f_{NF} and f_F represent the non-fossil and fossil fraction respectively and are determined by ^{14}C measurements.
α is determined by linear regression between levoglucosan and TC_{NF} (see 3.2);
D_X represent partitioning factors, the indices stand for the type of carbon source this factor is used (BB for Biomass Burning and F for Fossil);
D_{BB} is derived from the literature (see 3.3);
D_F is a function of EC/OC and EC_{BB}.
Both TC_{NF} and TC_{BB} are required to determine OC_{bio}.

2.2.3. Major ions and trace elements

The quantification of major ions (SO_4^{2-}, NO_3^-, NH_4^+, Na^+, K^+, Mg^{2+} and Ca^{2+}) was carried out by ion chromatography following methods described by Jaffrezo et al. (1998). Trace elements, such as calcium, aluminum, lead, copper, and others were analyzed by ICP-MS, following the method described in Waked et al. (2014). $PM_{2.5}$ concentration was estimated by mass balance, based on chemical composition *i.e.* the organic matter (OM, based on OC), elemental carbon, sulfate, nitrate and ammonium.

2.2.4. ^{14}C measurements and f_{NF}

Radiocarbon measurements are carried out using AixMICADAS, a compact AMS dedicated to the measurement of ultra-small samples (Synal et al., 2007; Bard et al., 2015). It is equipped with a hybrid ion source, which can handle both solid (graphite) and gaseous (CO_2) samples. AixMICADAS and its performances are described elsewhere (Bard et al., 2015; Tuna et al., 2018). For aerosol analysis, it is coupled to an elemental analyzer (Vario MicroCube, Elementar) by the Gas Interface System (GIS). The EA (Elemental Analyzer) combustion tube is filled with tungsten oxide granules and heated to 1050 °C; the reduction tube is composed of copper wires and silver wool, maintained at 550 °C.

A small piece of the impacted filter (0.95 cm^2) is generally sufficient for ^{14}C measurements in atmospheric PM, as a carbon mass of between 10 and 100 µgC is needed with the ion source in the gas mode (Bonvalot et al., 2016). The small sample punch is wrapped in a silver boat that has previously been prebaked at 800 °C for 2 h in order to limit organic contamination. The CO_2 obtained by combustion in the EA is collected and quantified by the GIS, before being injected into the ion source for the AMS measurement.

For each filter, two measurements were performed. The carbon mass (TC) was determined by the GIS with an overall error of 4% (Bonvalot et al., 2016). This error is based on the average difference between duplicated measurements of aerosol samples. It represents the overall uncertainty, including the measurement uncertainty of the GIS itself and is linked to possible heterogeneities of the sampled filters. This 4% uncertainty is propagated to all carbon mass values from the GIS.

Radiocarbon results are based on measured $^{14}C/^{12}C$ ratios, which are corrected for fractionation using the ^{13}C ion beam analyzed on a separate Faraday cup of AixMICADAS. Corrected ^{14}C data are then expressed as $F^{14}C$, a normalized activity equivalent to the modern fraction (Reimer et al., 2004), which does not depend on the year of measurement. The radiocarbon measurement protocol and contamination correction method are fully described in Bonvalot et al. (2016). The contamination brought by the EA and the silver boat is estimated at M_C = 1.45 ± 0.26 µgC, with a $F^{14}C_C$ of 0.73 ± 0.11 (confidence interval of 2σ). To calculate the sample mass (M_S) and the sample modern fraction ($F^{14}C_S$), the measured values (M_M and $F^{14}C_M$) are corrected for this contamination with the following formulas:

$$M_s = M_M - M_C$$

$$F^{14}C_S = \frac{F^{14}C_M \times M_M - F^{14}C_C \times M_C}{M_M - M_C} \quad (1)$$

$F^{14}C_S$ is then used to calculate the non-fossil fraction (f_{NF}). f_{NF} is the radiocarbon measurement normalized to a reference value ($f_{NF,ref}$), which considers the increase of atmospheric $F^{14}C$ resulting from the thermonuclear weapon tests of the late 1950s and early 1960s (Levin et al., 2010). According to Levin et al. (2013), the atmospheric radiocarbon value for the end of 2012 is around 1.04 $F^{14}C$, which is the value chosen for calculating our non-fossil fraction:

$$f_{NF} = \frac{F^{14}C_{Sample}}{f_{NF,ref}} \quad (2)$$

2.3. Source apportionment calculation methods

Sources of carbonaceous aerosols are apportioned using the measured values of EC/TC, levoglucosan, TC and f_{NF} based on ^{14}C. These calculations are performed in two steps. The first step is carried out following the method described in Bonvalot et al. (2016), and provides the origins of the carbonaceous fraction. The second step, based on Salma et al. (2017), enables to go further in the attribution by distinguishing the OC fraction from the EC fraction. The different fractions of the carbonaceous aerosols are represented in Fig. 2:

2.3.1. Source apportionment of TC

- TC_{NF} and TC_F

Distinction between TC_F (fossil total carbon) and TC_{NF} (non-fossil total carbon) is performed as described in equations (3) and (4), by using the measured carbon concentration and the measured f_{NF}. The different factors in the equations are color coded. Terms in purple and bold represent experimental results on individual samples, and terms in black are calculation results.

$$TC_{NF} = \boldsymbol{f_{NF}} \times \boldsymbol{TC} \quad (3)$$

$$TC_F = f_F \times TC = (1 - \boldsymbol{f_{NF}}) \times \boldsymbol{TC} \quad (4)$$

TC_F is directly obtained from equation (4).

- TC_{BB} quantification

To quantify TC_{BB}, both levoglucosan concentration and a coefficient (α) are necessary. The α coefficient is determined by linear regression (least squares method) between TC_{NF} concentrations, determined by equation (3), and levoglucosan concentrations, using fall and winter measurements; the slope obtained in this linear regression is α. This value represents the TC/levoglucosan ratio linked purely to the biomass burning source, *i.e.* TC_{BB}/levoglucosan. The zero intercept, β,

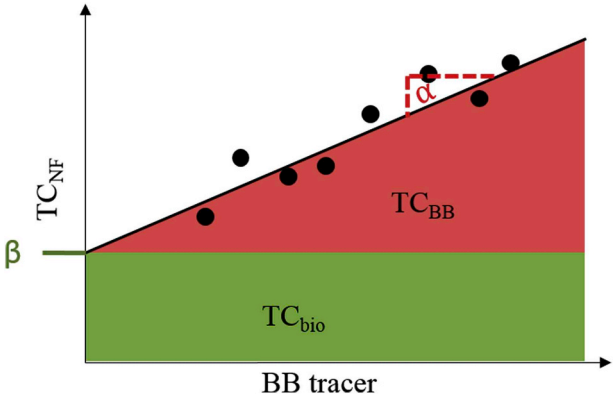

Fig. 3. Linear regression of TC_{NF} vs. levoglucosan: $TC_{NF} = \alpha$ x lévo + β. Representation of α and β determination.

represents the biogenic emission background which is assumed to be constant for a given season. A schematic of this principle is detailed in Fig. 3.

Both α and β take into account the uncertainties on TC_{NF}, which are based on ^{14}C measurements and on levoglucosan concentration (estimated at around ± 10% with a 95% confidence factor). By using the α coefficient and the individual levoglucosan concentration, as exposed in equation (5), TC_{BB} can be calculated for each sample.

$$TC_{BB} = \alpha \times \boldsymbol{levo} \quad (5)$$

TC_{BB} values are thus derived from both a molecular tracer and TC_{NF} values, which are themselves derived from ^{14}C analyses.

- TC_{bio} quantification

The biogenic fraction has a $F^{14}C$ that should be close to the atmospheric $F^{14}C$ at the time of emission, which corresponds to the time of sample collection within a few weeks at most. By contrast, biomass burning is mainly based on wood that grew over a few decades, a timespan characterized by a gradual $F^{14}C$ decrease in the atmosphere since the thermonuclear bomb tests of the early 1960s. This implies that wood carbon has a mean $F^{14}C$ slightly higher than that of the atmosphere at the time of aerosol sampling. We have adopted the average $F^{14}C_{BB}$ of 1.10 proposed by Lewis et al. (2004) and Szidat et al. (2006), based on atmospheric ^{14}C evolution and a tree growth model. To quantify the biogenic fraction of TC_{NF}, the following mass balance equation is used:

$$\begin{aligned} TC \times F^{14}C_S &= TC_{BB} \times F^{14}C_{BB} + TC_{bio} \times F^{14}C_{bio} + TC_F \times F^{14}C_F \\ &= TC_{BB} \times F^{14}C_{BB} + TC_{bio} \times F^{14}C_{bio} \end{aligned} \quad (6)$$

- TC, carbon concentration determined with the GIS [μg m^{-3}],
- $F^{14}C_S$ measured in the sample,
- TC_{BB}, carbon concentration from biomass burning (based on the levoglucosan measurement and determination of α) [μg m^{-3}],
- $F^{14}C_{BB}$, modern fraction of 1.10 assumed for the wood used in biomass burning,
- TC_{bio}, carbon concentration from biogenic emissions [μg m^{-3}],
- $F^{14}C_{bio}$, modern fraction of 1.04 for biogenic emissions,
- TC_F, carbon concentration from fossil sources [μg m^{-3}],
- $F^{14}C_F$, modern fraction of 0 for the fossil emissions devoid of ^{14}C.

From equation (6), it is possible to derive TC_{bio} as follows:

$$\begin{aligned} TC_{bio} &= \frac{TC \times F^{14}C_S - TC_{BB} \times F^{14}C_{BB}}{F^{14}C_{bio}} \\ &= \frac{\boldsymbol{TC} \times \boldsymbol{F^{14}C_S} - \alpha \times \boldsymbol{levo} \times F^{14}C_{BB}}{F^{14}C_{bio}} \end{aligned} \quad (7)$$

As in previous equations, the different origins of factors are color-coded. Terms in purple and in bold represent experimental results on individual samples. The term in green and in bold originates from correlation between experimental data; terms in blue stand for values from the literature.

Determined by linear regression between TC_{NF} in function of levoglucosan (see Fig. 3), the β factor also give an estimation of the mean TC_{bio}.

It should be noted that the $f_{NF,ref}$ value used to determine f_{NF}, and therefore TC_{NF} and TC_F, is set to the atmospheric level (1.04 $F^{14}C$), as we assumed the non-fossil source to be purely biogenic. However, the non-fossil carbon is composed of biogenic and biomass burning fractions, which differ slightly in their $^{14}C/^{12}C$ ratios. Ideally, both should be acknowledged in the definition of $f_{NF,ref}$. Zhang et al. (2012) and Zotter et al. (2014) have taken into account both $F^{14}C_{bio}$ and $F^{14}C_{BB}$ in f_{NF}, by assuming their respective contributions. In Bonvalot et al. (2016), we set $f_{NF,ref} = F^{14}C_{bio} = 1.04$ for summer samples but $f_{NF,ref} = F^{14}C_{BB} = 1.10$ for winter samples because the levoglucosan winter levels were very high (mean value around 3 μg m^{-3}, and up to 8.5 μg m^{-3}) and the β value was indistinguishable, indicating negligible biogenic emissions during winter in these valleys.

Fos-sur-Mer can be viewed as an intermediate case as levoglucosan levels remains moderate in winter. It is thus difficult to make a priori assumptions about the TC_{bio}/TC_{NF} ratio before the calculation. Nevertheless, the above determinations allow the a posteriori calculation of a more accurate $f_{NF,ref}$ value in winter, with 1.08, which is close to the 1.04 assumed in the calculation. Using the new $f_{NF,ref}$ value would change the TC_{NF} and TC_F by only 4%, which is small compared to other measurement uncertainties.

2.3.2. Source apportionment of EC and OC

The relative contributions of EC and OC to the TC fraction are estimated following the same approach as in Salma et al. (2017), which is also similar to those proposed by Gelencsér et al. (2007) and Gilardoni et al. (2011) and close to Yttri et al. (2011b). The measurements of radiocarbon and levoglucosan are used together with the EC/TC ratio determined by thermo-optical analysis. As a necessary complement in the calculation, we use a constant value for the OC_{BB}/levoglucosan as given by the literature (Salma et al., 2017).

- EC_{BB} and OC_{BB}

TC_{BB} is composed of EC_{BB} and OC_{BB} which can be estimated using the partitioning factor D_{BB}, as defined below:

$$D_{BB} = \frac{\left(OC_{BB}/levo\right) \times \left(EC/OC\right)_{BB}}{\alpha} \quad (8)$$

$$\begin{aligned} EC_{BB} &= D_{BB} \times TC_{BB} \\ OC_{BB} &= TC_{BB} - EC_{BB} \end{aligned} \quad (9)$$

The term in green ()α originates from the correlation between experimental data; ratio terms in blue stand for values from the literature.

- α, slope determined by linear regression between the measured levo and TC_{NF} (see Fig. 5),
- OC_{BB}/levo ratio of 5.59 ± 1.68, following work by Salma et al. (2017). This value is compatible with a variety of wood types used in Austria (Schmidl et al., 2008).
- $(EC/OC)_{BB}$ ratio of 0.17 ± 0.009 following work by Salma et al. (2017), which is compatible with values of 0.16 ± 0.01 and 0.18 ± 0.01, as used by Szidat et al. (2006) and Bernardoni et al. (2013), respectively.

- OC_{bio}

The OC_{bio} fraction originates from vegetal emissions, without

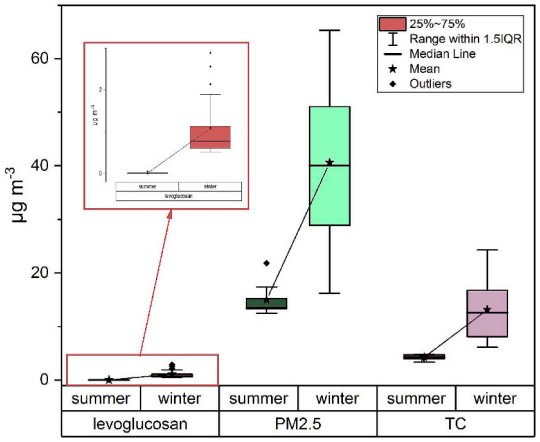

Fig. 4. Box plot representation of levoglucosan, $PM_{2.5}$ and TC concentrations for summer and winter.

combustion. Because $EC_{bio} = 0$, OC_{bio} corresponds to TC_{bio}. OC_{bio} is partly composed of secondary organic aerosols (SOAs), which are of mixed origin from fossil and non-fossil carbon fractions. SOAs are formed in the atmosphere by the transfer to the particle phase of VOCs (Volatile Organic Compounds) oxidized in the gas phase by atmospheric oxidant species (notably OH, O_3). Biogenic gaseous emissions consist mostly of isoprene, monoterpenes and sesquiterpenes, which are considered as the most important biogenic SOA precursors (Hallquist et al., 2009; Kanakidou et al., 2005).

- EC_F and OC_F

TC_F is composed of EC_F and OC_F, which can be estimated using a partitioning factor D_F, as defined below:

$$D_F = \frac{\left(\frac{EC}{TC}\right) - \frac{EC_{BB}}{TC}}{1 - f_{NF}} \quad 10$$

Bold purple terms represents experimental results on individual samples. The term in black originates from a previous calculation (equation (9)).

- (EC/TC) ratio as measured with the Sunset thermal-optical measurements,
- EC_{BB} calculated previously [µg m^{-3}],
- TC measured with the GIS during the ^{14}C analysis [µg m^{-3}],
- f_{NF} deduced from ^{14}C measurements.

$$EC_F = D_F \times TC_F$$
$$OC_F = TC_F - EC_F \quad 11$$

The OC_F fraction is composed of both primary (POC_F) and secondary organic aerosols (SOC_F). Fossil SOAs are formed by oxidation and condensation of exhaust gases, and can represent an important part of total SOAs (Huang et al., 2014).

3. Results and discussion

3.1. $PM_{2.5}$ composition

$PM_{2.5}$ concentration in the air varies significantly with the season, as illustrated in Fig. 4. During the warm season (July and August 2013), the average concentration is about 15 µg m^{-3} (SD = 3 µg m^{-3}, N = 9), which is below the French goal limit (25 µg m^{-3}, in average per year) but higher than the WHO recommended value (10 µg m^{-3}). The mean and median $PM_{2.5}$ for summer samples is close to that determined by El Haddad et al. (2011) for the summer of 2008 in Marseille. For the winter, the average $PM_{2,5}$ concentration is around 41 µg m^{-3} (median = 40 µg m^3, SD = 14 µg m^{-3}, N = 20), significantly greater than the regulatory threshold for warning the general public.

The proportion of carbon (TC) in the $PM_{2.5}$ is fairly constant at about 30% throughout the year (33% during winter and 29% during summer, see Fig. 4) with TC amounts for the fall/winter reaching a mean concentration of 13 µgC m^{-3} (median = 13 µg m^{-3}, SD = 6 µgC m^{-3}, N = 20) and of 4 µgC m^{-3} (median = 4 µg m^{-3}, SD = 1 µgC m^{-3}, N = 9) in the summer.

Seasonality was also observed in other European Mediterranean cities by Salameh et al. (2015), with similar TC concentration in Marseille (located about 40 km from Fos-sur-Mer) and Thessaloniki (one of the major harbors of the Aegean Sea).

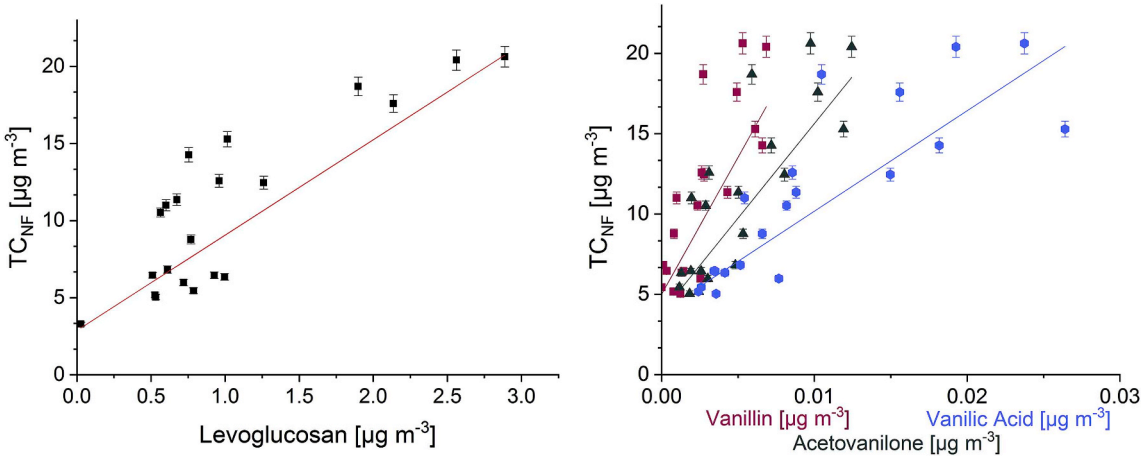

Fig. 5. (a) Linear regression of TC_{NF} vs. levoglucosan. $TC_{NF} = \alpha$ x lévo + β:
α = 6.6 ± 1.5;
β = 2.5 ± 1.3;
Pearson's r = 0.714, Adjusted R^2 = 0.482.
(b) Linear regression of TC_{NF} vs.three other BB tracers (vanillin, acetovanilone, vanillic acid).
TC_{NF} = A x $tracer_{BB}$ + B:
$A_{vanillin}$ = 1703.4 ± 347.4 $B_{vanillin}$ = 5.0 ± 0.7 Pearson's r = 0.756, Adjusted R^2 = 0.548;
$A_{acetovanilone}$ = 1178.5 ± 206.6 $B_{acetovanilone}$ = 3.9 ± 0.8 Pearson's r = 0.802, Adjusted R^2 = 0.624;
$A_{vanilic\ acid}$ = 625.5 ± 90.7 $B_{vanilic\ acid}$ = 3.9 ± 0.7 Pearson's r = 0.852, Adjusted R^2 = 0.710.

Levoglucosan average concentrations by season are also represented in Fig. 4. During summer, levoglucosan concentrations remain low (mean concentration = 17 ng m^{-3}, median = 13 ng m^{-3}, SD = 11 ng m^{-3}, N = 9). Those concentrations are close, for example, to European summer levels described in different studies (Giannoni et al., 2012; Jedynska et al., 2015; Puxbaum et al., 2007; Yttri et al., 2011a). They are also in the same range as concentrations measured in Marseille during summer 2008 (El Haddad et al., 2011). The impact of biomass burning during summer can thus be considered as very weak, even if levoglucosan can only give an estimation.

For the fall/winter samples, levels of levoglucosan are about 70 times higher than for summer (mean concentration = 1.1 µg m^{-3}, median concentration = 0.8 µg m^{-3}, SD = 0.8 µg m^{-3}, N = 20), which is greater than all winter/summer ratios reported by Puxbaum et al. (2007). Strong seasonal patterns were also detected in several European cities such as Oslo, Munich and Granada (Jedynska et al., 2015; Titos et al., 2017). Even if Fos-sur-Mer is a small town in itself (16 000 inhabitants) the same pattern than major cities is obtained. This can be explained by the fact that it is located in a widely populated area in proximity to industries. Nevertheless, winter levels of levoglucosan in Fos-sur-Mer remain lower than those detected in winter in French and Swiss alpine valleys, which suffer from strong pollution periods due to biomass combustion (Favez et al., 2009; Zotter et al., 2014; Bonvalot et al., 2016). These alpine valleys are enclosed between steep slopes and are characterized by temperature inversions which limit atmospheric mixing during winter. These specific meteorological conditions are not experienced in Fos-sur-Mer.

The non-fossil carbon fraction presents a seasonality with a f_{NF} of 0.83 during the fall/winter and a f_{NF} of 0.59 for the summer. A similar pattern is observed in locations with important atmospheric pollution, located in South Europe along the Mediterranean Sea, such as the Po Valley, Italy (Gilardoni et al., 2011), Barcelona, Spain (Minguillón et al., 2011) and Milan, Italy (Bernardoni et al., 2013).

3.2. Total carbon source apportionment

The carbonaceous fraction is mostly composed of TC_{NF}, even if it varies during seasons (see Table 1). This contrasts with the TC_F concentrations, which remains constant over the whole year. TC_{NF} can originate from two major sources: biomass burning and biogenic emissions from natural sources, such as plants and trees, or marine biological sources but also from anthropogenic sources such as cooking emissions. Both fractions are composed of primary organic aerosols (POAs) and secondary organic aerosols (SOAs) (Hallquist et al., 2009).

Firstly, the α coefficient is determined as described in paragraph 2.3.1. As shown in Fig. 5, a α slope of 6.6 ± 1.5 is obtained, which is roughly equivalent to the values obtained for Passy (6.0 ± 0.2) and Chamonix (5.9 ± 0.3), both located in the French Alps (Bonvalot et al., 2016). The α value for Fos-sur-Mer is also within the TC_{BB}/levo range (4.3 and 17.2) based on experimental studies performed by Schmidl et al. (2008).

TC_{bio} results determined by the mass balance equation (see equation (7)) are listed in, the Supplemental Data Table. The mean winter concentration of TC_{bio} is 3.6 µg m^{-3} (median = 2.9 µg m^{-3}, SD = 2.9 µg m^{-3}, N = 20), which is compatible with the β value of 2.5 ± 1.3 µg m^{-3} determined in Fig. 5(a).

Levoglucosan is probably the most widely used molecular tracer for biomass burning because its concentration represents a significant proportion of OA_{BB} for fresh emissions (about 15–50%, depending of the nature of combustion, as described by Bertrand et al. (2018a)). In our case, levoglucosan represents between 4 and 13% of the total OM (Organic Matter) for winter samples. However, others BB tracers (Simoneit, 2002) like vanillin, acetovanillone and vanillic acid (methoxyphenols) can be considered. These compounds present are both primary and secondary, which provides information on the BB contribution in aging aerosols. In the case of Fos-sur-Mer, the concentrations of these compounds are small (less than 0.03 µg m^{-3} for each of them) and their sum represents less than 0.3% of winter-time OM. Despite their small concentrations, they are useful BB tracers, complementary to levoglucosan.

Linear regressions between TC_{NF} and vanillin, acetovanillone, or vanillic acid are all statistically significant (Pearson'r = 0.76 to 0.85, adjusted R^2 = 0.55 to 0.73). Apparent differences of the linear slopes for the three methoxyphenols (Fig. 5(b)) may be related to their different secondary enrichments during aging of the aerosols. Fig. 5(b) also shows that the three linear regressions converge towards a similar zero intercept (3.9–5.0 ± 0.7 µgC) which is compatible with the value found for the TC_{NF}-levoglucosan regression (2.5 ± 1.3 µgC). Overall, this confirms our average TC_{bio} estimation around 3 µg m^{-3}.

3.3. Organic carbon (OC) elemental carbon (EC) source apportionment and seasonal variation

Following the approach explained in section 2.3.2, the OC and EC contributions for each carbon source are determined and results are listed in the Supplemental Data Table.

For fall and winter, the major contributors to the carbonaceous particles are OC_{BB} (45%) and EC_{BB} (8%) whereas they only represent 2% and 0.4% respectively for the warm season (see Fig. 6). The concentrations also drastically vary with 6.1 µg m^{-3} of OC_{BB} and 1.0 µg m^{-3} of EC_{BB} in winter and only 0.1 and 0.01 µg m^{-3} respectively in summer, as exposed in Fig. 7.

The very weak influence of biomass burning during summer in Fos-sur-Mer, when the dry and hot weather frequently leads to wildfires in the region, confirms that the main source of TC_{BB} is linked to wood burning for residential heating.

Nevertheless, the importance of biomass burning during winter could be surprising because Fos-sur-Mer is located in the south of France with relatively mild winters. However frequent cold episodes linked to strong northerly winds may increase the need for temporary residential heating based on open fire wood burning.

Similar contributions of wood burning are typically observed for colder regions such as alpine valleys (Bonvalot et al., 2016; Zotter et al., 2014) or in the Czech city of Mladá Boleslav (Hovorka et al., 2015). BB winter level obtained in our study is also superior to the one measured in Zurich (Szidat et al., 2006). However, in these colder regions, wood

Table 1
Statistical details for OC_F, EC_F, OC_{BB}, EC_{BB} ans OC_{bio}.

	OC_F [µg m^{-3}]		EC_F [µg m^{-3}]		OC_{BB} [µg m^{-3}]		EC_{BB} [µg m^{-3}]		OC_{bio} [µg m^{-3}]	
	Cold Season	Warm Season	Cold Season	Warm Season	Cold Season	Warm Season	Cold Season	Warm Season	Cold Season	Warm Season
Mean	1.0	0.9	1.1	0.9	6.1	0.1	1.0	0.0	3.6	2.5
Median	1.0	0.8	0.8	0.9	4.4	0.1	0.7	0.0	2.9	2.6
Percentile 25	0.3	0.7	0.6	0.7	3.4	0.0	0.6	0.0	1.3	2.0
Percentile 75	1.5	1.0	1.3	1.1	6.0	0.1	1.0	0.0	6.1	2.7
Minimum	0.0	0.6	0.0	0.6	2.9	0.0	0.5	0.0	0.0	1.6
Maximum	2.6	1.8	3.8	1.2	16.2	0.3	2.7	0.0	9.0	3.3

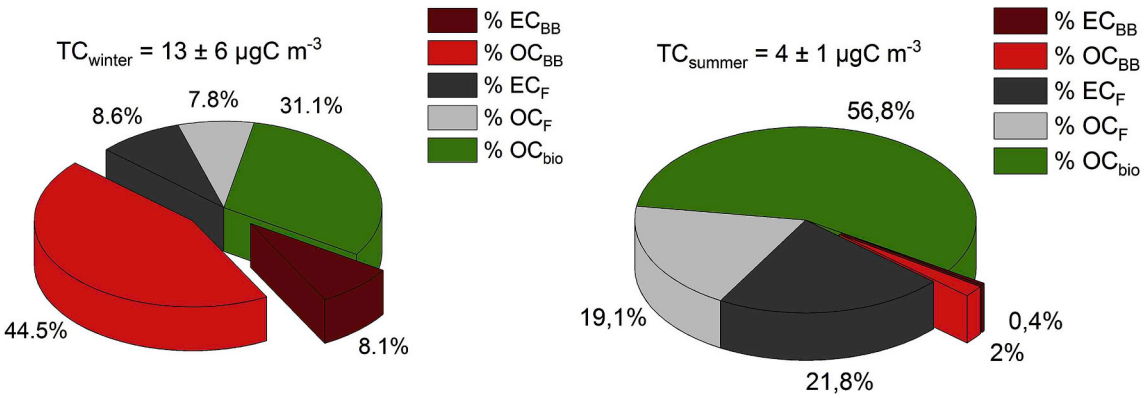

Fig. 6. Proportional contributions to carbonaceous aerosols for fall/winter 2012–13 (a) and summer 2013 (b).

is usually burnt in closed fireplaces and woodstoves, whereas open fireplaces are frequent in the Provence Region where Fos-sur-Mer is located. In addition, green waste burning and agricultural combustion burning (notably from rice fields in the Camargue and vine shoots) may have also contributed to this fraction during the fall. The summer BB fraction could also partly originate from ash spread on agricultural fields as soil fertilizer. Further research is needed to quantify these hypothetic contributions.

In the Mediterranean area, similar result is obtained in Marseille, during winter where the main contribution to OA (Organic Aerosol) is also biomass burning (BB) which contribute to 48% of the OA. On the contrary, in Barcelona (Spain) the proportion of OC_{BB} remains constant on a yearly basis; for winter OC_{BB} represents 35% of OC_{NF} and 33% in summer which correspond to 17–21% of the total OC (Minguillón et al., 2011).

The fossil contribution also varies between the cold and warm seasons, with 9% of EC_F and 8% of OC_F in winter and 22% EC_F and 19% OC_F in summer. However, concentration of EC_F and OC_F remain constant (about 1 µg m^{-3} for EC_F and OC_F for both winter and summer). Relative contributions of the fossil fraction to TC are exposed in Fig. 6 and the concentrations are detailed in Fig. 7. The stability of the fossil carbon concentrations (OC_F, EC_F) is compatible with the stability of the vehicular traffic throughout the year. An additional contribution could be EC sediment in soils over the years, which is subjected to re-suspension with the crustal fraction.

An examination of EC during fall/winter reveals that half of it comes from biomass burning emissions, while the remainder is from fossil fuel combustion. Such an important contribution of biomass burning in EC was not observed in Milan where about 85% of EC was shown to originate from fossil sources (Bernardoni et al., 2013). In Barcelona (Spain), also a Mediterranean city, the fossil fraction of EC represents for 87% in winter and 91% in summer (Minguillón et al., 2011). For Montseny, located at 50 km of Barcelona in a forested area (720 m a.s.l), EC fossil percentage is smaller (66% in winter and 79% in summer). By contrast to winter, most summer EC (98%) in Fos-sur-Mer originates from fossil sources because biomass burning is very much reduced during the hot season.

The city of Ispra in northern Italy bears some similarities with Fos-sur-Mer in terms of industries and traffic. As reported by Gilardoni et al. (2011), the PM from Ispra presents similar seasonal patterns, with 12% of EC_F, 15% of OC_F, 11% of EC_{BB}, 53% of OC_{BB}, 9% of OC_{bio} in winter and 18% of EC_F, 15% of OC_F, 1% of EC_{BB}, 8% of OC_{BB}, 50% of OC_{bio} in summer. Hence, the importance of biomass burning is even greater during winter in Ispra (11 + 53 = 64%) than in Fos-sur-Mer (45 + 8 = 53%). The difference may be due to slightly colder temperatures in Ispra than in Fos-sur-Mer (climatological DJF averages of 2.5 °C and 6.5 °C, respectively, https://fr.climate-data.org/location/7679/).

The biogenic fraction (OC_{bio}) represents 57% of the total carbon during summer. During the cold season, OC_{bio} still represents more than a quarter of the total carbon. The mean and median values of TC_{bio} (= OC_{bio}) remain stable during fall/winter and summer, respectively 3.6 µgC m^{-3} (median = 2.9 µg m^{-3}, SD = 2.9 µg m^{-3}, N = 20) and 2.4 µgC m^{-3} (median = 2.6 µg m^{-3}, SD = 0.5 µg m^{-3}, N = 9), both equivalent to the β factor (2.5 ± 1.3 µg m^{-3}). See Figs. 6 and 7 and Table 1 for seasonal contributions and concentrations respectively.

OC_{bio} origins (and more specially winter OC_{bio}) are multiple and complex and can be both primary and secondary. The POC_{bio} (Primary OC_{bio}) can be related to cooking emissions and to direct biogenic emissions from the vegetation, with compounds like cellulose (Asslanian et al., 2018), particulate abrasion produced from leaf surface, fungal spores, monosaccharides, and others. For example, Bozzetti et al. (2016) have shown that for the rural site of Payerne (Switzerland), Primary Biologic Organic Aerosols (PBOAs) are comparable to the SOA contribution in the coarse organic matter (yearly average of 37%, with 19% in winter and 60% in summer). Similar results are obtained in French rural sites (Golly et al., 2019).

The contribution of SOC_{bio} (Secondary OC_{bio}) could be important, as observed in Paris (France) during winter (Beekmann et al., 2015) and Marseille where OOA (Oxygenated Organic Aerosol, *i.e.* aged aerosol directly associated to SOA) represents 63% of the OA during summer (Bozzetti et al., 2017).

SOC_{bio} could partly be linked to secondary aerosols from biomass burning emissions (SOA_{BB}) (Bertrand et al., 2018a). However, the OC_{BB}/levoglucosan ratios from the literature are usually estimated with atmospheric samples which are already aged (SOA_{BB} would be included, at least partly, in our calculation of the OC_{BB} fraction). SOC_{bio} could also originates from cooking emissions, biogenic, agricultural emissions.

The stability of TC_{bio} may seem surprising because biological emissions by vegetation is enhanced during the warm season (Bozzetti et al., 2016; Bonvalot et al., 2016). Windy conditions during winter and fall may also favor the production and transport of primary particles. In addition, secondary particles originating from the aging of BB emissions may possibly represent an important fraction of the OC_{bio} fraction. Bertrand et al. (2018a) have shown the importance of SOA_{BB} formation (up to 7 times the initial OA concentration after 6 h of photo chemical oxidation) and the influence of the aging onto the aerosol composition.

In order to distinguish SOAs and POAs, it is useful to compare TC_{bio} with molecular markers such as malic acid and DL-glyceric acid, which are obtained by oxidation of biogenic compounds, such as biogenic fatty acids and n-alkanes. Fig. 8 reports significant correlations between TC_{bio} and both organic acids during summer, thus confirming the importance of SOAs. Those correlations seem linear and don't seem to follow the exponential model described by Leaitch et al. (2011), but a larger dataset is probably needed to detect a statistical difference

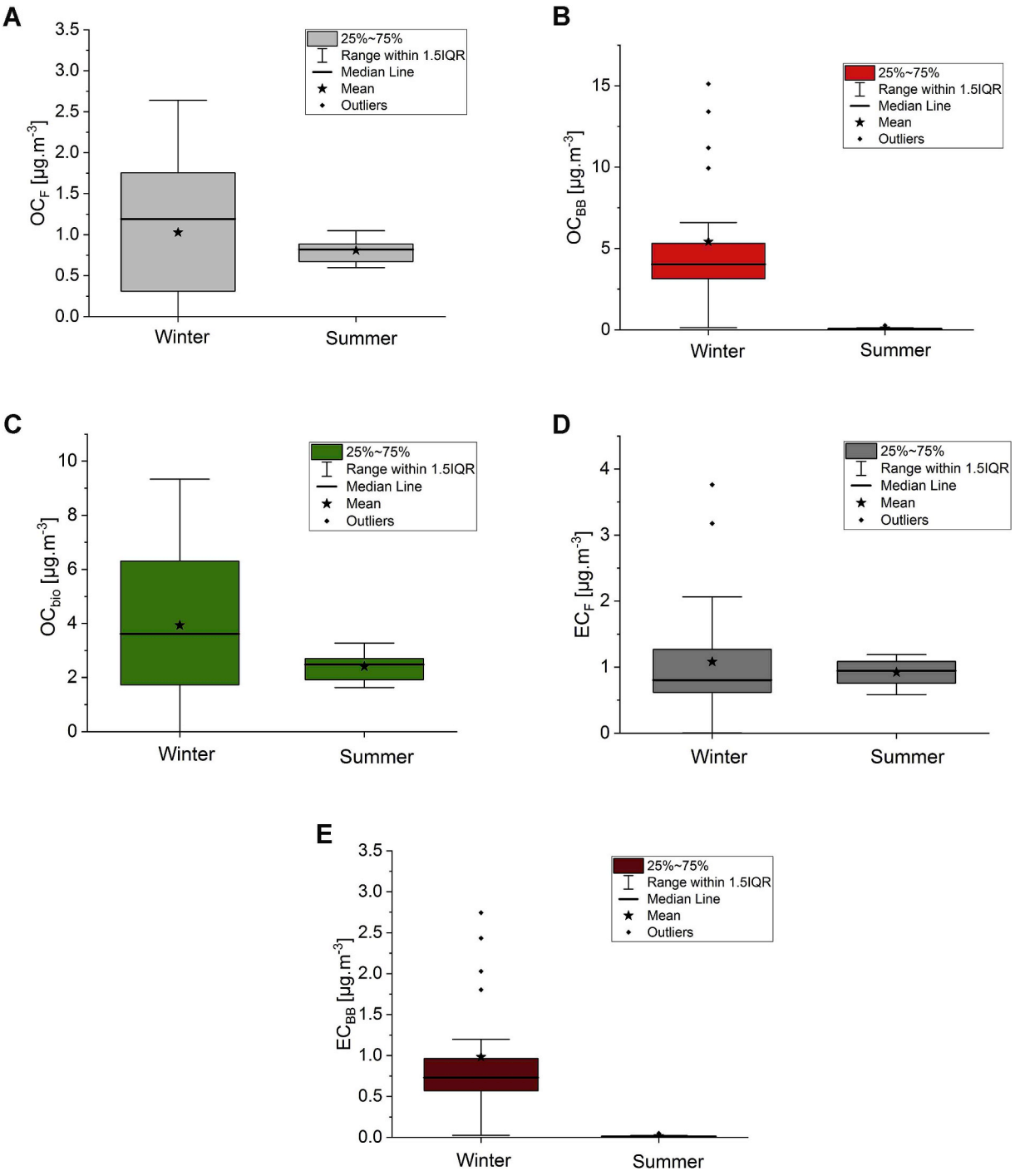

Fig. 7. Box plots of carbonaceous fractions a) OC_F, b) OC_{BB}, c) OC_{Bio}, d) EC_F and e) EC_{BB}.

between the two types of monotonic evolution. In any case, the observed correlations are compatible with the conclusions by El Haddad et al. (2013) who identified the presence during summer in Marseille of OOAs (Oxygenated Organic Aerosols) - commonly related to SOAs (Jimenez et al., 2009) - contributing to non-fossil sources.

Interestingly, both zero intercepts of the linear regressions are significantly different from zero ($1.7 \pm 0.3\,\mu g\,m^{-3}$ in Fig. 8 (a) and $2.0 \pm 0.2\,\mu g\,m^{-3}$ in Fig. 8 (b)), which also points to the presence of POAs, amounting to about one third to one half of TC_{bio}. By contrast, malic acid levels are low in winter, and neither malic nor DL-glyceric acid are correlated with TC_{bio}. This is compatible with the hypothesis that TC_{bio} in winter is mainly linked to production and transport of POAs. Hence, the apparent stability of TC_{bio} regardless of season may be due to the seasonality of fluxes and SOA/POA ratios of emissions by vegetation.

4. Conclusions

Carbonaceous aerosols from the heavily industrialized Fos-sur-Mer region are apportioned using a multi-proxy approach. Origins of the fractions in $PM_{2.5}$ samples are determined by using ^{14}C results combined with the EC/OC ratio, levoglucosan and methoxyphenols (biomass combustion proxies) and selected fatty acids (biogenic emission proxies). Samples collected in the summer and fall/winter periods of 2013 indicate that carbonaceous material represents about 30% of the $PM_{2.5}$ fraction. Our multi-proxy approach provides information on the

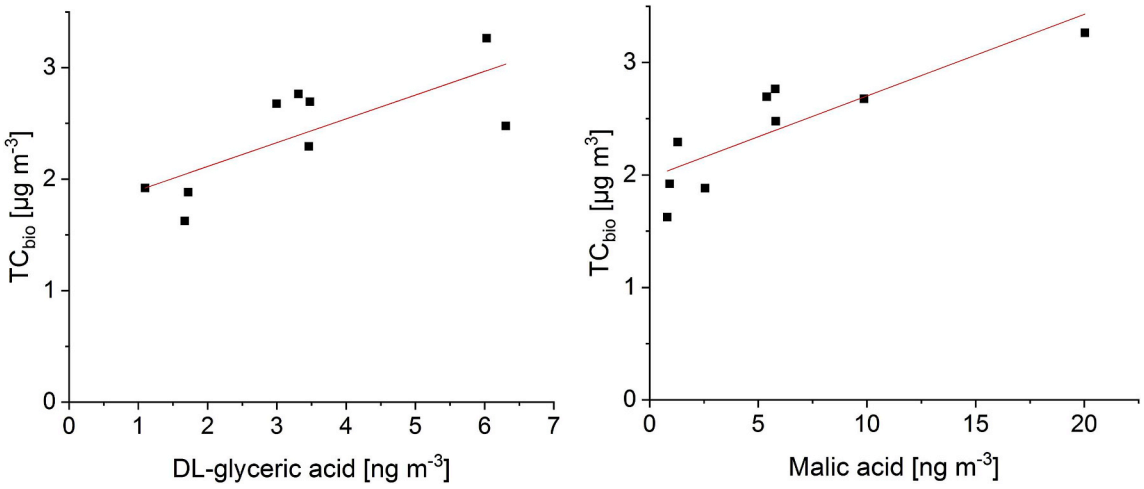

Fig. 8. Correlation between OCbio and (a) DL glyceric acid Pearson's R = 0.749 (b) malic acid Pearson's R = 0.853, for summer samples.

main sources of pollutants and their seasonal variations:

- A strong seasonality is detected for carbonaceous particle concentrations (TC) for the 30 studied samples, levoglucosan, methoxyphenols and the non-fossil carbon fraction based on ^{14}C (f_{NF}), pointing towards the influence of biomass burning (BB) for domestic heating as the main source during winter.
- The TC_{NF} and levoglucosan concentration are 3 times and 70 times respectively, larger in the 20 winter samples than during the warm season (10 samples), and the observed concentrations allow to estimate that BB in fall and winter contribute to ≈ 53% of the total carbonaceous aerosols, and ≈63% of the non-fossil carbon).
- While BB is clearly dominant in winter, it remains very low during the warm season (≈2% of the total carbonaceous aerosols),
- A significant contribution of biogenic carbon (TC_{bio}) is quantified for both summer and winter samples. Comparison with biogenic molecular proxies suggests that primary and secondary aerosols are quantitatively important. The lack of seasonality of TC_{bio} may be due to variations of the relative proportions of primary and secondary organic aerosols, POAs being dominant (relatively, over SOAs) in winter while SOAs represent up to a half of TC_{bio} in summer.
- Fossil carbons (EC_F + OC_F) from industrial, shipping and vehicular sources are relatively higher in the 10 spring and summer samples. However, their absolute concentration is stable along all seasons, which is compatible with intense activity throughout the year.

This study provides important constraints on the composition and sources of the PM background in this populated region. Our multi-proxy approach based on ^{14}C and molecular tracers, allows to evidence a strong biomass burning contribution linked to residential heating in winter, high and stable inputs from traffic and industries throughout the year and significant biogenic contributions during both seasons.

Acknowledgements

AixMICADAS was acquired and is operated in the framework of the EQUIPEX project ASTER-CEREGE with additional matching funds from the Collège de France, which also supports the salaries of the authors from CEREGE. Analytical aspects at IGE were supported by the Air-O-Sol platform within Labex OSUG@2020 (ANR10 LABX56).

Appendix A. Supplementary data

Supplementary data to this article can be found online at https://doi.org/10.1016/j.atmosenv.2019.04.008.

References

Angove, D.E., Fookes, C.J.R., Hynes, R.G., Walters, C.K., Azzi, M., 2006. The characterisation of secondary organic aerosol formed during the photodecomposition of 1,3-butadiene in air containing nitric oxide. Atmos. Environ. 40, 4597–4607. https://doi.org/10.1016/j.atmosenv.2006.03.046.

Arndt, J., Sciare, J., Mallet, M., Roberts, G.C., Marchand, N., Sartelet, K., Sellegri, K., Dulac, F., Healy, R.M., Wenger, J.C., 2017. Sources and mixing state of summertime background aerosol in the north-western Mediterranean basin. Atmos. Chem. Phys. 17, 6975–7001. https://doi.org/10.5194/acp-17-6975-2017.

Asslanian, K., Weber, S., Jacob, V., Peter, C., Charron, A., Uzu, G., Favez, O., Albinet, A., Guillaud, G., Thomasson, A., Trebuchon, C., Jaffrezo, J.-L., 2018. Tracers of Primary and Secondary biogenic organic aerosol in a multi-sites PMF study at an urban scale. Atmos. Chem. Phys (in prep).

Bard, E., Tuna, T., Fagault, Y., Bonvalot, L., Wacker, L., Fahrni, S., Synal, H.-A., 2015. AixMICADAS, the accelerator mass spectrometer dedicated to 14C recently installed in Aix-en-Provence, France. In: Nucl. Instrum. Methods Phys. Res. Sect. B Beam Interact. Mater. At., the Thirteenth Accelerator Mass Spectrometry Conference, vol. 361. pp. 80–86. https://doi.org/10.1016/j.nimb.2015.01.075.

Beekmann, M., Prévôt, A.S.H., Drewnick, F., Sciare, J., Pandis, S.N., Denier van der Gon, H.A.C., Crippa, M., Freutel, F., Poulain, L., Ghersi, V., Rodriguez, E., Beirle, S., Zotter, P., von der Weiden-Reinmüller, S.-L., Bressi, M., Fountoukis, C., Petetin, H., Szidat, S., Schneider, J., Rosso, A., El Haddad, I., Megaritis, A., Zhang, Q.J., Michoud, V., Slowik, J.G., Moukhtar, S., Kolmonen, P., Stohl, A., Eckhardt, S., Borbon, A., Gros, V., Marchand, N., Jaffrezo, J.L., Schwarzenboeck, A., Colomb, A., Wiedensohler, A., Borrmann, S., Lawrence, M., Baklanov, A., Baltensperger, U., 2015. In situ, satellite measurement and model evidence on the dominant regional contribution to fine particulate matter levels in the Paris megacity. Atmos. Chem. Phys. 15, 9577–9591. https://doi.org/10.5194/acp-15-9577-2015.

Bernardoni, V., Calzolai, G., Chiari, M., Fedi, M., Lucarelli, F., Nava, S., Piazzalunga, A., Riccobono, F., Taccetti, F., Valli, G., Vecchi, R., 2013. Radiocarbon analysis on organic and elemental carbon in aerosol samples and source apportionment at an urban site in Northern Italy. J. Aerosol Sci., Special Issue. In: 10th International Conference on Carbonaceous Particles in the Atmosphere, Vienna, Austria, 2011, vol. 56. pp. 88–99. https://doi.org/10.1016/j.jaerosci.2012.06.001.

Bertrand, A., Stefenelli, G., Jen, C.N., Pieber, S.M., Bruns, E.A., Ni, H., Temime-Roussel, B., Slowik, J.G., Goldstein, A.H., Haddad, I.E., Baltensperger, U., Prévôt, A.S.H., Wortham, H., Marchand, N., 2018a. Evolution of the chemical fingerprint of biomass burning organic aerosol during aging. Atmos. Chem. Phys. 18, 7607–7624. https://doi.org/10.5194/acp-18-7607-2018.

Bertrand, A., Stefenelli, G., Pieber, S.M., Bruns, E.A., Temime-Roussel, B., Slowik, J.G., Wortham, H., Prévôt, A.S.H., Haddad, I.E., Marchand, N., 2018b. Influence of the vapor wall loss on the degradation rate constants in chamber experiments of levoglucosan and other biomass burning markers. Atmos. Chem. Phys. Discuss. 1–29. https://doi.org/10.5194/acp-2018-40.

Birch, M.E., Cary, R.A., 1996. Elemental carbon-based method for monitoring occupational exposures to particulate diesel exhaust. Aerosol Sci. Technol. 25, 221–241. https://doi.org/10.1080/02786829608965393.

Bonvalot, L., Tuna, T., Fagault, Y., Jaffrezo, J.-L., Jacob, V., Chevrier, F., Bard, E., 2016. Estimating contributions from biomass burning, fossil fuel combustion, and biogenic carbon to carbonaceous aerosols in the Valley of Chamonix: a dual approach based on radiocarbon and levoglucosan. Atmos. Chem. Phys. 16, 13753–13772. https://doi.org/10.5194/acp-16-13753-2016.

Bozzetti, C., Daellenbach, K.R., Hueglin, C., Fermo, P., Sciare, J., Kasper-Giebl, A., Mazar, Y., Abbaszade, G., El Kazzi, M., Gonzalez, R., Shuster-Meiseles, T., Flasch, M., Wolf, R., Křepelová, A., Canonaco, F., Schnelle-Kreis, J., Slowik, J.G., Zimmermann, R., Rudich, Y., Baltensperger, U., El Haddad, I., Prévôt, A.S.H., 2016. Size-resolved identification, characterization, and quantification of primary biological organic aerosol at a european rural site. Environ. Sci. Technol. 50, 3425–3434. https://doi.org/10.1021/acs.est.5b05960.

Bozzetti, C., El Haddad, I., Salameh, D., Daellenbach, K.R., Fermo, P., Gonzalez, R., Minguillón, M.C., Iinuma, Y., Poulain, L., Elser, M., Müller, E., Slowik, J.G., Jaffrezo,

J.-L., Baltensperger, U., Marchand, N., Prévôt, A.S.H., 2017. Organic aerosol source apportionment by offline-AMS over a full year in Marseille. Atmos. Chem. Phys. 17, 8247–8268. https://doi.org/10.5194/acp-17-8247-2017.
Caseiro, A., Bauer, H., Schmidl, C., Pio, C.A., Puxbaum, H., 2009. Wood burning impact on PM10 in three Austrian regions. Atmos. Environ. 43, 2186–2195. https://doi.org/10.1016/j.atmosenv.2009.01.012.
Cavalli, F., Viana, M., Yttri, K.E., Genberg, J., Putaud, J.-P., 2010. Toward a standardised thermal-optical protocol for measuring atmospheric organic and elemental carbon: the EUSAAR protocol. Atmos Meas Tech 3, 79–89. https://doi.org/10.5194/amt-3-79-2010.
Chung, S.H., Seinfeld, J.H., 2002. Global distribution and climate forcing of carbonaceous aerosols. J. Geophys. Res. Atmospheres 107, 4407. https://doi.org/10.1029/2001JD001397.
Claeys, M., Graham, B., Vas, G., Wang, W., Vermeylen, R., Pashynska, V., Cafmeyer, J., Guyon, P., Andreae, M.O., Artaxo, P., Maenhaut, W., 2004. formation of secondary organic aerosols through photooxidation of isoprene. Science 303, 1173–1176. https://doi.org/10.1126/science.1092805.
Currie, L.A., 2000. Evolution and multidisciplinary frontiers of 14C aerosol science. Radiocarbon 42, 115–126.
Dron, J., Chamaret, P., Marchand, N., Temime-Roussel, B., Ravier, S., Sylvestre, A., Wortham, H., 2017. Variabilité physico-chimique des épisodes de pollution atmosphérique à proximité de la zone industrialo-portuaire de Fos-sur-Mer. Pollut. Atmos. 233, 1–13. http://lodel.irevues.inist.fr/pollution-atmospherique/index.php?id=6081.
Dusek, U., Hitzenberger, R., Kasper-Giebl, A., Kistler, M., Meijer, H.A.J., Szidat, S., Wacker, L., Holzinger, R., Röckmann, T., 2017. Sources and formation mechanisms of carbonaceous aerosol at a regional background site in The Netherlands: insights from a year-long radiocarbon study. Atmos. Chem. Phys. 17, 3233–3251. https://doi.org/10.5194/acp-17-3233-2017.
El Haddad, I., Marchand, N., Dron, J., Temime-Roussel, B., Quivet, E., Wortham, H., Jaffrezo, J.L., Baduel, C., Voisin, D., Besombes, J.L., Gille, G., 2009. Comprehensive primary particulate organic characterization of vehicular exhaust emissions in France. Atmos. Environ. 43, 6190–6198. https://doi.org/10.1016/j.atmosenv.2009.09.001.
El Haddad, I., Marchand, N., Wortham, H., Piot, C., Besombes, J.-L., Cozic, J., Chauvel, C., Armengaud, A., Robin, D., Jaffrezo, J.-L., 2011. Primary sources of PM2.5 organic aerosol in an industrial Mediterranean city, Marseille. Atmos. Chem. Phys. 11, 2039–2058. https://doi.org/10.5194/acp-11-2039-2011.
El Haddad, I., D'Anna, B., Temime-Roussel, B., Nicolas, M., Boreave, A., Favez, O., Voisin, D., Sciare, J., George, C., Jaffrezo, J.-L., Wortham, H., Marchand, N., 2013. Towards a better understanding of the origins, chemical composition and aging of oxygenated organic aerosols: case study of a Mediterranean industrialized environment, Marseille. Atmos. Chem. Phys. 13, 7875–7894. https://doi.org/10.5194/acp-13-7875-2013.
Favez, O., Cachier, H., Sciare, J., Sarda-Estève, R., Martinon, L., 2009. Evidence for a significant contribution of wood burning aerosols to PM2.5 during the winter season in Paris, France. Atmos. Environ. 43, 3640–3644. https://doi.org/10.1016/j.atmosenv.2009.04.035.
Fuzzi, S., Baltensperger, U., Carslaw, K., Decesari, S., Denier van der Gon, H., Facchini, M.C., Fowler, D., Koren, I., Langford, B., Lohmann, U., Nemitz, E., Pandis, S., Riipinen, I., Rudich, Y., Schaap, M., Slowik, J.G., Spracklen, D.V., Vignati, E., Wild, M., Williams, M., Gilardoni, S., 2015. Particulate matter, air quality and climate: lessons learned and future needs. Atmos. Chem. Phys. 15, 8217–8299. https://doi.org/10.5194/acp-15-8217-2015.
Gelencsér, A., 2004. Major carbonaceous particle types and their sources. In: Carbonaceous Aerosol, Atmospheric and Oceanic Sciences Library. Springer.
Gelencsér, A., May, B., Simpson, D., Sánchez-Ochoa, A., Kasper-Giebl, A., Puxbaum, H., Caseiro, A., Pio, C., Legrand, M., 2007. Source apportionment of PM2.5 organic aerosol over Europe: primary/secondary, natural/anthropogenic, and fossil/biogenic origin. J. Geophys. Res. Atmospheres 112, D23S04. https://doi.org/10.1029/2006JD008094.
Giannoni, M., Martellini, T., Del Bubba, M., Gambaro, A., Zangrando, R., Chiari, M., Lepri, L., Cincinelli, A., 2012. The use of levoglucosan for tracing biomass burning in PM2.5 samples in Tuscany (Italy). Environ. Pollut. 167, 7–15. https://doi.org/10.1016/j.envpol.2012.03.016.
Gilardoni, S., Vignati, E., Cavalli, F., Putaud, J.P., Larsen, B.R., Karl, M., Stenström, K., Genberg, J., Henne, S., Dentener, F., 2011. Better constraints on sources of carbonaceous aerosols using a combined 14C – macro tracer analysis in a European rural background site. Atmos. Chem. Phys. 11, 5685–5700. https://doi.org/10.5194/acp-11-5685-2011.
Goix, S., Dron, J., Raucau, A., Chamaret, P., 2017. Lancement de l'étude de bio-surveillance des populations exposées aux émissions atmosphériques à proximité de la zone industrialo-portuaire de Fos-sur-Mer (INDEX). Pollut. Atmos. 233 4 pages. http://lodel.irevues.inist.fr/pollution-atmospherique/index.php?id=5214.
Golly, B., Waked, A., Weber, S., Samaké, A., Jacob, V., Conil, S., Rangonio, J., Chrétien, E., Vagnot, M.P., Robic, P.Y., Besombes, J.-L., Jaffrezo, J.-L., 2019. Organic markers and OC source apportionment for seasonal variations of PM2.5 at 5 rural sites in France. Atmos. Environ. 198, 142–157. https://www.sciencedirect.com/science/article/pii/S1352231018307179.
Goriaux, M., Jourdain, B., Temime, B., Besombes, J.-L., Marchand, N., Albinet, A., Leoz-Garziandia, E., Wortham, H., 2006. Field comparison of particulate PAH measurements using a low-flow denuder device and conventional sampling systems. Environ. Sci. Technol. 40 (20), 6398–6404. https://doi.org/10.1021/es060544m.
Hallquist, M., Wenger, J.C., Baltensperger, U., Rudich, Y., Simpson, D., Claeys, M., Dommen, J., Donahue, N.M., George, C., Goldstein, A.H., Hamilton, J.F., Herrmann, H., Hoffmann, T., Iinuma, Y., Jang, M., Jenkin, M.E., Jimenez, J.L., Kiendler-Scharr, A., Maenhaut, W., McFiggans, G., Mentel, T.F., Monod, A., Prévôt, A.S.H., Seinfeld, J.H., Surratt, J.D., Szmigielski, R., Wildt, J., 2009. The formation, properties and impact of secondary organic aerosol: current and emerging issues. Atmos. Chem. Phys. 9, 5155–5236. https://doi.org/10.5194/acp-9-5155-2009.
Heal, M.R., Naysmith, P., Cook, G.T., Xu, S., Duran, T.R., Harrison, R.M., 2011. Application of 14C analyses to source apportionment of carbonaceous PM2.5 in the UK. Atmos. Environ. 45, 2341–2348. https://doi.org/10.1016/j.atmosenv.2011.02.029.
Hennigan, C.J., Sullivan, A.P., Collett, J.L., Robinson, A.L., 2010. Levoglucosan stability in biomass burning particles exposed to hydroxyl radicals. Geophys. Res. Lett. 37, L09806. https://doi.org/10.1029/2010GL043088.
Hovorka, J., Pokorná, P., Hopke, P.K., Křůmal, K., Mikuška, P., Píšová, M., 2015. Wood combustion, a dominant source of winter aerosol in residential district in proximity to a large automobile factory in Central Europe. Atmos. Environ. 113, 98–107. https://doi.org/10.1016/j.atmosenv.2015.04.068.
Hsieh, L.-Y., Kuo, S.-C., Chen, C.-L., Tsai, Y.I., 2007. Origin of low-molecular-weight dicarboxylic acids and their concentration and size distribution variation in suburban aerosol. Atmos. Environ. 41, 6648–6661. https://doi.org/10.1016/j.atmosenv.2007.04.014.
Hua, Q., Barbetti, M., Rakowski, A.Z., 2013. Atmospheric radiocarbon for the period 1950–2010. Radiocarbon 55, 2059–2072. https://doi.org/10.2458/azu_js_rc.v55i2.16177.
Huang, R.-J., Zhang, Y., Bozzetti, C., Ho, K.-F., Cao, J.-J., Han, Y., Daellenbach, K.R., Slowik, J.G., Platt, S.M., Canonaco, F., Zotter, P., Wolf, R., Pieber, S.M., Bruns, E.A., Crippa, M., Ciarelli, G., Piazzalunga, A., Schwikowski, M., Abbaszade, G., Schnelle-Kreis, J., Zimmermann, R., An, Z., Szidat, S., Baltensperger, U., Haddad, I.E., Prévôt, A.S.H., 2014. High secondary aerosol contribution to particulate pollution during haze events in China. Nature 514, 218–222. https://doi.org/10.1038/nature13774.
Jaffrezo, J.L., Calas, N., Bouchet, M., 1998. Carboxylic acids measurements with ionic chromatography. Atmos. Environ. 32, 2705–2708. https://doi.org/10.1016/S1352-2310(98)00026-0.
Jedynska, A., Hoek, G., Wang, M., Eeftens, M., Cyrys, J., Beelen, R., Cirach, M., De Nazelle, A., Keuken, M., Visschedijk, A., Nystad, W., Akhlaghi, H.M., Meliefste, K., Nieuwenhuijsen, M., de Hoogh, K., Brunekreef, B., Kooter, I.M., 2015. Spatial variations of levoglucosan in four European study areas. Sci. Total Environ. 505, 1072–1081. https://doi.org/10.1016/j.scitotenv.2014.10.091.
Jimenez, J.L., Canagaratna, M.R., Donahue, N.M., Prevot, A.S.H., Zhang, Q., Kroll, J.H., DeCarlo, P.F., Allan, J.D., Coe, H., Ng, N.L., Aiken, A.C., Docherty, K.S., Ulbrich, I.M., Grieshop, A.P., Robinson, A.L., Duplissy, J., Smith, J.D., Wilson, K.R., Lanz, V.A., Hueglin, C., Sun, Y.L., Tian, J., Laaksonen, A., Raatikainen, T., Rautiainen, J., Vaattovaara, P., Ehn, M., Kulmala, M., Tomlinson, J.M., Collins, D.R., Cubison, M.J.,E., Dunlea, J., Huffman, J.A., Onasch, T.B., Alfarra, M.R., Williams, P.I., Bower, K., Kondo, Y., Schneider, J., Drewnick, F., Borrmann, S., Weimer, S., Demerjian, K., Salcedo, D., Cottrell, L., Griffin, R., Takami, A., Miyoshi, T., Hatakeyama, S., Shimono, A., Sun, J.Y., Zhang, Y.M., Dzepina, K., Kimmel, J.R., Sueper, D., Jayne, J.T., Herndon, S.C., Trimborn, A.M., Williams, L.R., Wood, E.C., Middlebrook, A.M., Kolb, C.E., Baltensperger, U., Worsnop, D.R., 2009. Evolution of organic aerosols in the atmosphere. Science 326, 1525–1529. https://doi.org/10.1126/science.1180353.
Jordan, T.B., Seen, A.J., Jacobsen, G.E., 2006. Levoglucosan as an atmospheric tracer for woodsmoke. Atmos. Environ. 40, 5316–5321. https://doi.org/10.1016/j.atmosenv.2006.03.023.
Kanakidou, M., Seinfeld, J.H., Pandis, S.N., Barnes, I., Dentener, F.J., Facchini, M.C., Van Dingenen, R., Ervens, B., Nenes, A., Nielsen, C.J., Swietlicki, E., Putaud, J.P., Balkanski, Y., Fuzzi, S., Horth, J., Moortgat, G.K., Winterhalter, R., Myhre, C.E.L., Tsigaridis, K., Vignati, E., Stephanou, E.G., Wilson, J., 2005. Organic aerosol and global climate modelling: a review. Atmos. Chem. Phys. 5, 1053–1123. https://doi.org/10.5194/acp-5-1053-2005.
Kawamura, K., Bikkina, S., 2016. A review of dicarboxylic acids and related compounds in atmospheric aerosols: molecular distributions, sources and transformation. Atmos. Res. 170, 140–160. https://doi.org/10.1016/j.atmosres.2015.11.018.
Kawamura, K., Seméré, R., Imai, Y., Fujii, Y., Hayashi, M., 1996. Water soluble dicarboxylic acids and related compounds in Antarctic aerosols. J. Geophys. Res. Atmospheres 101, 18721–18728. https://doi.org/10.1029/96JD01541.
Kim, D., Jung, J., Lee, H., Choi, S.-H., Lee, S., Oh, S., 2016. Characterization of sampling artifacts in the measurement of carbonaceous particles using high- and low-volume samplers in Daejeon, Korea. Atmos. Environ. 139, 157–166. https://doi.org/10.1016/j.atmosenv.2016.05.029.
Leaitch, W.R., Macdonald, A.M., Brickell, P.C., Liggio, J., Sjostedt, S.J., Vlasenko, A., Bottenheim, J., Huang, L., Li, S.-M., Liu, P.S.K., Toom-Sauntry, D., Hayden, K.A., Sharma, S., Shantz, N.C., Wiebe, H.A., Zhang, W., Abbatt, J.P.D., Slowik, J.G., Chang, R.Y.-W., Russell, L.M., Schwartz, R.E., Takahama, S., Jayne, J.T., Ng, N.L., 2011. Temperature response of the submicron organic aerosol from temperate forests. Atmos. Environ. 45, 6696–6704. https://doi.org/10.1016/j.atmosenv.2011.08.047.
Lelieveld, J., Evans, J.S., Fnais, M., Giannadaki, D., Pozzer, A., 2015. The contribution of outdoor air pollution sources to premature mortality on a global scale. Nature 525, 367–371. https://doi.org/10.1038/nature15371.
Lelieveld, J., Klingmüller, K., Pozzer, A., Pöschl, U., Fnais, M., Daiber, A., Münzel, T., 2019. Cardiovascular disease burden from ambient air pollution in Europe reassessed using novel hazard ratio functions. Eur. Heart J. 0, 1–7. https://doi.org/10.1093/eurheartj/ehz135.
Levin, I., Kromer, B., Hammer, S., 2013. Atmospheric Δ 14 CO2 trend in Western European background air from 2000 to 2012. Tellus B 65. https://doi.org/10.3402/tellusb.v65i0.20092.
Levin, I., Naegler, T., Kromer, B., Diehl, M., Francey, R.J., Gomez-Pelaez, A.J., Steele, L.P., Wagenbach, D., Weller, R., Worthy, D.E., 2010. Observations and modelling of the global distribution and long-term trend of atmospheric 14 CO 2. Tellus B 62, 26–46. https://doi.org/10.1111/j.1600-0889.2009.00446.x.
Lewis, C.W., Klouda, G.A., Ellenson, W.D., 2004. Radiocarbon measurement of the biogenic contribution to summertime PM-2.5 ambient aerosol in Nashville. TN. Atmos. Environ. 38, 6053–6061. https://doi.org/10.1016/j.atmosenv.2004.06.011.
Mader, B.T., Pankow, J.F., 2000. Gas/solid partitioning of semivolatile organic compounds (SOCs) to air filters. 1. Partitioning of polychlorinated dibenzodioxins, polychlorinated dibenzofurans and polycyclic aromatic hydrocarbons to teflon membrane filters. Atmos. Environ. 34 (28), 4879–4887. https://doi.org/10.1016/

S1352-2310(00)00241-7.
Martinsson, J., Abdul Azeem, H., Sporre, M.K., Bergström, R., Ahlberg, E., Öström, E., Kristensson, A., Swietlicki, E., Eriksson Stenström, K., 2017. Carbonaceous aerosol source apportionment using the Aethalometer model – evaluation by radiocarbon and levoglucosan analysis at a rural background site in southern Sweden. Atmos. Chem. Phys. 17, 4265–4281. https://doi.org/10.5194/acp-17-4265-2017.
Michoud, V., Sciare, J., Sauvage, S., Dusanter, S., Léonardis, T., Gros, V., Kalogridis, C., Zannoni, N., Féron, A., Petit, J.-E., Crenn, V., Baisnée, D., Sarda-Estève, R., Bonnaire, N., Marchand, N., DeWitt, H.L., Pey, J., Colomb, A., Gheusi, F., Szidat, S., Stavroulas, I., Borbon, A., Locoge, N., 2017. Organic carbon at a remote site of the western Mediterranean Basin: sources and chemistry during the ChArMEx SOP2 field experiment. Atmos. Chem. Phys. 17, 8837–8865. https://doi.org/10.5194/acp-17-8837-2017.
Minguillón, M.C., Pérez, N., Marchand, N., Bertrand, A., Temime-Roussel, B., Agrios, K., Szidat, S., Drooge, B. van, Sylvestre, A., Alastuey, A., Reche, C., Ripoll, A., Marco, E., Grimalt, J.O., Querol, X., 2016. Secondary organic aerosol origin in an urban environment: influence of biogenic and fuel combustion precursors. Faraday Discuss 189, 337–359. https://doi.org/10.1039/C5FD00182J.
Minguillón, M.C., Perron, N., Querol, X., Szidat, S., Fahrni, S.M., Alastuey, A., Jimenez, J.L., Mohr, C., Ortega, A.M., Day, D.A., Lanz, V.A., Wacker, L., Reche, C., Cusack, M., Amato, F., Kiss, G., Hoffer, A., Decesari, S., Moretti, F., Hillamo, R., Teinilä, K., Seco, R., Peñuelas, J., Metzger, A., Schallhart, S., Müller, M., Hansel, A., Burkhart, J.F., Baltensperger, U., Prévôt, A.S.H., 2011. Fossil versus contemporary sources of fine elemental and organic carbonaceous particulate matter during the DAURE campaign in Northeast Spain. Atmos. Chem. Phys. 11, 12067–12084. https://doi.org/10.5194/acp-11-12067-2011.
Nolte, C.G., Schauer, J.J., Cass, G.R., Simoneit, B.R.T., 2001. Highly polar organic compounds present in wood smoke and in the ambient atmosphere. Environ. Sci. Technol. 35, 1912–1919. https://doi.org/10.1021/es001420r.
Penner, J.E., Chuang, C.C., Grant, K., 1998. Climate forcing by carbonaceous and sulfate aerosols. Clim. Dyn. 14, 839–851. https://doi.org/10.1007/s003820050259.
Pope, C.A.I., Dockery, D.W., 2006. Health effects of fine particulate air pollution: lines that connect. J. Air Waste Manag. Assoc. 56, 709–742. https://doi.org/10.1080/10473289.2006.10464485.
Pöschl, U., 2005. Atmospheric aerosols: composition, transformation, climate and health effects. Angew. Chem. Int. Ed. 44, 7520–7540. https://doi.org/10.1002/anie.200501122.
Putaud, J.-P., Raes, F., Van Dingenen, R., Brüggemann, E., Facchini, M.-C., Decesari, S., Fuzzi, S., Gehrig, R., Hüglin, C., Laj, P., Lorbeer, G., Maenhaut, W., Mihalopoulos, N., Müller, K., Querol, X., Rodriguez, S., Schneider, J., Spindler, G., Brink, H. ten, Tørseth, K., Wiedensohler, A., 2004. A European aerosol phenomenology—2: chemical characteristics of particulate matter at kerbside, urban, rural and background sites in Europe. Atmos. Environ. 38, 2579–2595. https://doi.org/10.1016/j.atmosenv.2004.01.041.
Putaud, J.-P., Van Dingenen, R., Alastuey, A., Bauer, H., Birmili, W., Cyrys, J., Flentje, H., Fuzzi, S., Gehrig, R., Hansson, H.C., Harrison, R.M., Herrmann, H., Hitzenberger, R., Hüglin, C., Jones, A.M., Kasper-Giebl, A., Kiss, G., Kousa, A., Kuhlbusch, T.A.J., Löschau, G., Maenhaut, W., Molnar, A., Moreno, T., Pekkanen, J., Perrino, C., Pitz, M., Puxbaum, H., Querol, X., Rodriguez, S., Salma, I., Schwarz, J., Smolik, J., Schneider, J., Spindler, G., ten Brink, H., Tursic, J., Viana, M., Wiedensohler, A., Raes, F., 2010. A European aerosol phenomenology – 3: physical and chemical characteristics of particulate matter from 60 rural, urban, and kerbside sites across Europe. Atmos. Environ. 44, 1308–1320. https://doi.org/10.1016/j.atmosenv.2009.12.011.
Puxbaum, H., Caseiro, A., Sánchez-Ochoa, A., Kasper-Giebl, A., Claeys, M., Gelencsér, A., Legrand, M., Preunkert, S., Pio, C., 2007. Levoglucosan levels at background sites in Europe for assessing the impact of biomass combustion on the European aerosol background. J. Geophys. Res. Atmospheres 112, D23S05. https://doi.org/10.1029/2006JD008114.
Ramanathan, V., Crutzen, P.J., Kiehl, J.T., Rosenfeld, D., 2001a. Aerosols, climate, and the hydrological cycle. Science 294, 2119–2124. https://doi.org/10.1126/science.1064034.
Ramanathan, V., Crutzen, P.J., Lelieveld, J., Mitra, A.P., Althausen, D., Anderson, J., Andreae, M.O., Cantrell, W., Cass, G.R., Chung, C.E., Clarke, A.D., Coakley, J.A., Collins, W.D., Conant, W.C., Dulac, F., Heintzenberg, J., Heymsfield, A.J., Holben, B., Howell, S., Hudson, J., Jayaraman, A., Kiehl, J.T., Krishnamurti, T.N., Lubin, D., McFarquhar, G., Novakov, T., Ogren, P.K., Podgorny, I.A., Prather, K., Priestley, K., Prospero, J.M., Quinn, P.K., Rajeev, K., Rasch, P., Rupert, S., Sadourny, R., Satheesh, S.K., Shaw, G.E., Sheridan, P., Valero, F.P.J., 2001b. Indian Ocean Experiment: an integrated analysis of the climate forcing and effects of the great Indo-Asian haze. J. Geophys. Res. 106, 28371–28398.
Reimer, P.J., Brown, T.A., Reimer, R.W., 2004. Discussion: reporting and calibration of post-bomb 14C data. Radiocarbon 46, 1299–1304. https://doi.org/10.2458/azu_js_rc.46.4183.
Salameh, D., Detournay, A., Pey, J., Pérez, N., Liguori, F., Saraga, D., Bove, M.C., Brotto, P., Cassola, F., Massabò, D., Latella, A., Pillon, S., Formenton, G., Patti, S., Armengaud, A., Piga, D., Jaffrezo, J.L., Bartzis, J., Tolis, E., Prati, P., Querol, X., Wortham, H., Marchand, N., 2015. PM2.5 chemical composition in five European Mediterranean cities: a 1-year study. Atmos. Res. 155, 102–117. https://doi.org/10.1016/j.atmosres.2014.12.001.
Salma, I., Németh, Z., Weidinger, T., Maenhaut, W., Claeys, M., Molnár, M., Major, I., Ajtai, T., Utry, N., Bozóki, Z., 2017. Source apportionment of carbonaceous chemical species to fossil fuel combustion, biomass burning and biogenic emissions by a coupled radiocarbon–levoglucosan marker method. Atmos. Chem. Phys. 17, 13767–13781. https://doi.org/10.5194/acp-17-13767-2017.
Schauer, J.J., Kleeman, M.J., Cass, G.R., Simoneit, B.R.T., 2001. Measurement of emissions from air pollution sources. 3. C1 − C29 organic compounds from fireplace combustion of wood. Environ. Sci. Technol. 35, 1716–1728. https://doi.org/10.1021/es001331e.
Schmidl, C., Marr, I.L., Caseiro, A., Kotianová, P., Berner, A., Bauer, H., Kasper-Giebl, A., Puxbaum, H., 2008. Chemical characterisation of fine particle emissions from wood stove combustion of common woods growing in mid-European Alpine regions. Atmos. Environ. 42, 126–141. https://doi.org/10.1016/j.atmosenv.2007.09.028.
Simoneit, B.R.T., 2002. Biomass burning — a review of organic tracers for smoke from incomplete combustion. Appl. Geochem. 17, 129–162. https://doi.org/10.1016/S0883-2927(01)00061-0.
Simoneit, B.R.T., Schauer, J.J., Nolte, C.G., Oros, D.R., Elias, V.O., Fraser, M.P., Rogge, W.F., Cass, G.R., 1999. Levoglucosan, a tracer for cellulose in biomass burning and atmospheric particles. Atmos. Environ. 33, 173–182. https://doi.org/10.1016/S1352-2310(98)00145-9.
Sylvestre, A., Mizzi, A., Mathiot, S., Masson, F., Jaffrezo, J.L., Dron, J., Mesbah, B., Wortham, H., Marchand, N., 2017. Comprehensive chemical characterization of industrial PM2.5 from steel industry activities. Atmos. Environ. 152, 180–190. https://doi.org/10.1016/j.atmosenv.2016.12.032.
Sylvestre, A., 2017. Caractérisation de l'aérosol industriel et quantification de sa contribution aux PM 2.5 atmosphériques. Aix Marseille Université.
Synal, H.-A., Stocker, M., Suter, M., 2007. MICADAS: a new compact radiocarbon AMS system. Nucl. Instrum. Methods Phys. Res. Sect. B Beam Interact. Mater. At., Accelerator Mass Spectrometry Proceedings of the Tenth International Conference on Accelerator Mass Spectrometry 259, 7–13. https://doi.org/10.1016/j.nimb.2007.01.138.
Szidat, S., Jenk, T.M., Synal, H.-A., Kalberer, M., Wacker, L., Hajdas, I., Kasper-Giebl, A., Baltensperger, U., 2006. Contributions of fossil fuel, biomass-burning, and biogenic emissions to carbonaceous aerosols in Zurich as traced by 14C. J. Geophys. Res. Atmospheres 111, D07206. https://doi.org/10.1029/2005JD006590.
Szidat, S., Ruff, M., Perron, N., Wacker, L., Synal, H.-A., Hallquist, M., Shannigrahi, A.S., Yttri, K.E., Dye, C., Simpson, D., 2009. Fossil and non-fossil sources of organic carbon (OC) and elemental carbon (EC) in Göteborg, Sweden. Atmos. Chem. Phys. 9, 1521–1535. https://doi.org/10.5194/acp-9-1521-2009.
Titos, G., del Águila, A., Cazorla, A., Lyamani, H., Casquero-Vera, J.A., Colombi, C., Cuccia, E., Gianelle, V., Močnik, G., Alastuey, A., Olmo, F.J., Alados-Arboledas, L., 2017. Spatial and temporal variability of carbonaceous aerosols: assessing the impact of biomass burning in the urban environment. Sci. Total Environ. 578, 613–625. https://doi.org/10.1016/j.scitotenv.2016.11.007.
Tuna, T., Fagault, Y., Bonvalot, L., Capano, M., Bard, E., 2018. Development of small CO2 gas measurements with AixMICADAS. Nucl. Instrum. Methods Phys. Res. B 437, 93–97. https://doi.org/10.1016/j.nimb.2018.09.012.
Viana, M., Chi, X., Maenhaut, W., Cafmeyer, J., Querol, X., Alastuey, A., Mikuška, P., Vecera, Z., 2006. Influence of sampling artefacts on measured PM, OC, and EC levels in carbonaceous aerosols in an urban area. Aerosol Sci. Technol. 40, 107–117. https://doi.org/10.1080/02786820500484388.
Waked, A., Favez, O., Alleman, L.Y., Piot, C., Petit, J.-E., Delaunay, T., Verlinden, E., Golly, B., Besombes, J.-L., Jaffrezo, J.-L., Leoz-Garziandia, E., 2014. Source apportionment of PM10 in a north-western Europe regional urban background site (Lens, France) using positive matrix factorization and including primary biogenic emissions. Atmos. Chem. Phys. 14, 3325–3346. https://doi.org/10.5194/acp-14-3325-2014.
Yttri, K.E., Schnelle-Kreis, J., Maenhaut, W., Abbaszade, G., Alves, C., Bjerke, A., Bonnier, N., Bossi, R., Claeys, M., Dye, C., Evtyugina, M., García-Gacio, D., Hillamo, R., Hoffer, A., Hyder, M., Iinuma, Y., Jaffrezo, J.-L., Kasper-Giebl, A., Kiss, G., López-Mahia, P.L., Pio, C., Piot, C., Ramirez-Santa-Cruz, C., Sciare, J., Teinilä, K., Vermeylen, R., Vicente, A., Zimmermann, R., 2015. An intercomparison study of analytical methods used for quantification of levoglucosan in ambient aerosol filter samples. Atmos Meas Tech 8, 125–147. https://doi.org/10.5194/amt-8-125-2015.
Yttri, K.E., Simpson, D., Nøjgaard, J.K., Kristensen, K., Genberg, J., Stenström, K., Swietlicki, E., Hillamo, R., Aurela, M., Bauer, H., Offenberg, J.H., Jaoui, M., Dye, C., Eckhardt, S., Burkhart, J.F., Stohl, A., Glasius, M., 2011a. Source apportionment of the summer time carbonaceous aerosol at Nordic rural background sites. Atmos. Chem. Phys. 11, 13339–13357. https://doi.org/10.5194/acp-11-13339-2011.
Yttri, K.E., Simpson, D., Stenström, K., Puxbaum, H., Svendby, T., 2011b. Source apportionment of the carbonaceous aerosol in Norway - quantitative estimates based on 14C, thermal-optical and organic tracer analysis. Atmos. Chem. Phys. 11, 9375–9394. https://doi.org/10.5194/acp-11-9375-2011.
Zhang, T., Claeys, M., Cachier, H., Dong, S., Wang, W., Maenhaut, W., Liu, X., 2008. Identification and estimation of the biomass burning contribution to Beijing aerosol using levoglucosan as a molecular marker. Atmos. Environ. 42, 7013–7021. https://doi.org/10.1016/j.atmosenv.2008.04.050.
Zhang, Y.L., Perron, N., Ciobanu, V.G., Zotter, P., Minguillón, M.C., Wacker, L., Prévôt, A.S.H., Baltensperger, U., Szidat, S., 2012. On the isolation of OC and EC and the optimal strategy of radiocarbon-based source apportionment of carbonaceous aerosols. Atmos. Chem. Phys. Discuss. 12, 17657–17702. https://doi.org/10.5194/acpd-12-17657-2012.
Zotter, P., Ciobanu, V.G., Zhang, Y.L., El-Haddad, I., Macchia, M., Daellenbach, K.R., Salazar, G.A., Huang, R.-J., Wacker, L., Hueglin, C., Piazzalunga, A., Fermo, P., Schwikowski, M., Baltensperger, U., Szidat, S., Prévôt, A.S.H., 2014. Radiocarbon analysis of elemental and organic carbon in Switzerland during winter-smog episodes from 2008 to 2012 – Part 1: source apportionment and spatial variability. Atmos. Chem. Phys. 14, 13551–13570. https://doi.org/10.5194/acp-14-13551-2014.